Effect of the $t\bar{t}$ threshold on electroweak parameters

Bernd A. Kniehl
Deutsches Elektronen-Synchrotron, Notkestrasse 85, 2000 Hamburg, Germany

Alberto Sirlin
Department of Physics, New York University, 4 Washington Place, New York, New York 10003
(Received 8 September 1992)

Threshold effects in $e^+e^- \to t\bar{t}$ induce contributions to key electroweak parameters such as $\Delta\rho$, Δr, and $\sin^2\theta_W$ beyond the scope of perturbative calculations of $O(\alpha)$ and $O(\alpha\alpha_s)$. We quantitatively analyze these effects using once-subtracted dispersion relations which manifestly satisfy relevant Ward identities. The derivation and properties of the dispersion relations are discussed at some length. We find that the threshold effects enhance the familiar perturbative $O(\alpha\alpha_s)$ corrections by between 25% and 40%, depending on the t-quark mass. The shift in the predicted value of the W-boson mass due to the threshold effects ranges from -8 MeV at $m_t=91$ GeV to -45 MeV at $m_t=250$ GeV.

PACS number(s): 13.65.+i, 11.20.Fm, 14.40.Jz

I. INTRODUCTION

Dispersion relations (DR's) provide a powerful tool for calculating higher-order radiative corrections. To evaluate a matrix element $\mathcal{T}_{fi}$, which describes the transition from an initial state i to a final state f via one or more loops, one can, in principle, adopt the following two-step procedure. In the first step, one constructs the imaginary part of $\mathcal{T}_{fi}$ for an arbitrary invariant mass $s=p_i^2$ by means of Cutkosky's rule [1]:

$$-i(\mathcal{T}_{fi}-\mathcal{T}_{if}^*)=\sum_n (2\pi)^4\delta^{(4)}(p_n-p_i)\mathcal{T}_{nf}^*\mathcal{T}_{ni}\ , \qquad (1.1)$$

which is a corollary of S-matrix unitarity. Here the summation extends over all kinematically allowed intermediate configurations n which can be obtained by cutting the original diagram into two pieces in such a way that one of them is connected to i and the other one to f (this also includes phase-space integrations) and p_i and p_n denote the four-momenta of i and n, respectively. In the second step, appealing to analyticity, one derives the desired real part of $\mathcal{T}_{fi}$ from a DR:

$$\mathrm{Re}\mathcal{T}_{fi}(s)=\frac{1}{\pi}\mathcal{P}\int_{s_{\min}}^{\infty} ds'\frac{\mathrm{Im}\mathcal{T}_{fi}(s')}{s'-s}\ , \qquad (1.2)$$

where $\mathcal{P}$ denotes the principal value of the integral and $s_{\min}=\min_n p_n^2$. Depending on the high-s behavior of $\mathrm{Im}\mathcal{T}_{fi}(s)$, the right-hand side (RHS) of Eq. (1.2) may not converge, and one may need to replace the upper limit of integration by a cutoff scale Λ^2 to regulate the ultraviolet divergence. Furthermore, in order to avoid the occurrence of spurious quadratic divergences, which violate basic physical principles such as gauge invariance, it may be necessary to employ a suitably subtracted DR. We shall return to this point later.

Dispersive techniques offer both technical and physical advantages. Within perturbation theory, they permit the reduction of two-loop calculations to standard one-loop problems plus phase-space and dispersion integrations, which can sometimes be performed analytically even if massive particles are involved [2,3]. This procedure can also be iterated to tackle three-loop problems [4]. On the other hand, dispersive methods can often be applied where pure perturbation theory is either not reliable or bound to break down. To this end, one exploits the fact that, by virtue of the optical theorem, the imaginary parts of the loop amplitudes are related to total cross sections, which can be determined experimentally as a function of s. Perhaps, the best-known example of this kind in electroweak physics is the estimation of the light-quark contributions to the photon vacuum polarization, and thus to $\alpha(M_Z^2)$, based on experimental data of $\sigma(e^+e^-\to\text{hadrons})$ [5,6]. This type of analysis can be extended both to higher orders in QED [7] and to a broader class of electroweak parameters [8].

Although loop amplitudes involving the top quark are mathematically well behaved, it is evident that interesting and possibly significant features associated with the $t\bar{t}$ threshold cannot be accommodated when the perturbation series is truncated at finite order. In particular, perturbation theory up to $O(\alpha\alpha_s)$ predicts a discontinuous steplike threshold behavior of $\sigma(e^+e^-\to t\bar{t})$, which is, of course, a rather unrealistic approximation. It is well known that for low m_t there should be a spectrum of narrow toponium (θ) resonances lying densely across the threshold region (for a review see Ref. [9]). Above $m_t\approx 130$ GeV the partial width of $t\to W^+b$ becomes so large that the revolution period of a $t\bar{t}$ bound state would exceed its lifetime, and the individual resonances are smeared out to a coherent structure [10–12]. From the above discussion it is obvious that a phenomenologically acceptable description of $\sigma(e^+e^-\to t\bar{t})$ produces contributions to the absorptive parts of the photon and Z-boson self-energies beyond the usual perturbative calculation of $O(\alpha\alpha_s)$. This suggests the use of the dispersive

calculus in order to evaluate the additional contributions to the real parts, which in turn induce shifts in various electroweak observables.

The influence of quarkonium resonances on a variety of electroweak parameters was studied a couple of years ago [13]. At that time, special attention was focused on the case $m_t \approx M_Z/2$, in which θ-Z mixing plays a dominant role. Meanwhile, the range $m_t < 91$ GeV has been excluded at the 95% confidence level [14] and the possibility that $m_t \gtrsim 200$ GeV still exists [15]. An interesting property of virtual heavy-top-quark effects in $O(\alpha\alpha_s)$ [3,16] and $O(\alpha^2)$ [17,18] on the ρ parameter [19] and Δr [5] is that they tend to reduce the m_t-dependent parts of the one-loop results and thus to screen the familiar nondecoupling. As a consequence, the m_t upper bound is relaxed to higher values. It is of great phenomenological interest to find out whether this trend is supported by the radiative corrections that arise from the departure of the $t\bar{t}$ threshold from the naive steplike shape.

It is the purpose of this paper to present a careful quantitative analysis of the influence of $t\bar{t}$ threshold effects on central electroweak quantities such as $\Delta\rho$, Δr, and $\sin^2\theta_W$, which, in conjunction with accurate M_W, CERN e^+e^- collider LEP, and neutral-current measurements, give important information concerning m_t and M_H. A crucial technical detail in this context is the use of a subtraction prescription for the DR which manifestly complies with basic Ward identities (WI's). We have proposed such a prescription in a previous paper [20]. This paper is organized as follows. In Sec. II, we establish the dispersive formalism generalizing the derivation of Ref. [20]. In Sec. III, we apply this formalism to study threshold effects. In Sec. IV, we describe our parametrizations of the $t\bar{t}$ threshold. In Sec. V, we present and discuss our numerical results. Our conclusions are summarized in Sec. VI.

II. DISPERSION RELATIONS

Let us consider the vacuum-polarization tensor of a gauge boson, with four-momentum q, induced by a pair of virtual fermions with masses m_1 and m_2:

$$\Pi^{V,A}_{\mu\nu}(q,m_1,m_2) = -i\int d^4x\, e^{iq\cdot x}\langle 0|T^*[J^{V,A}_\mu(x)J^{V,A\dagger}_\nu(0)]|0\rangle \ , \tag{2.1a}$$

where T^* denotes the covariant time-ordered product and $J^{V,A}_\mu(x)$ represents the vector and axial-vector currents in configuration space, respectively. Except for flavor-preserving vector currents, with $m_1 = m_2$, current conservation is explicitly broken by mass terms. Lorentz covariance implies

$$\Pi^{V,A}_{\mu\nu}(q,m_1,m_2) = \Pi^{V,A}(s,m_1,m_2)g_{\mu\nu} + \lambda^{V,A}(s,m_1,m_2)q_\mu q_\nu \ , \tag{2.1b}$$

where $s = q^2$. As a rule, only the transverse parts $\Pi^{V,A}(s,m_1,m_2)$ contribute significantly to amplitudes involving light external fermions, and we wish to derive suitable DR's to evaluate these functions. Contracting Eq. (2.1) on both sides with q^μ, one obtains

$$\Pi^{V,A}(s,m_1,m_2) = -s\lambda^{V,A}(s,m_1,m_2) + \Delta^{V,A}(s,m_1,m_2) \ , \tag{2.2a}$$

where $\Delta^{V,A}(s,m_1,m_2)$ is defined by

$$\int d^4x\, e^{iq\cdot x}\langle 0|T[\partial^\mu J^{V,A}_\mu(x)J^{V,A\dagger}_\nu(0)]|0\rangle \equiv \Delta^{V,A}(s,m_1,m_2)q_\nu \ . \tag{2.2b}$$

A number of papers [2,13] have made use of DR's to relate the $\Pi^{V,A}(s,m_1,m_2)$ functions to their imaginary parts. In Ref. [20] we proposed to use the WI of Eq. (2.2a) directly and to write DR's for $\lambda^{V,A}(s,m_1,m_2)$ and $\Delta^{V,A}(s,m_1,m_2)$. This procedure eliminates the quadratic divergences present in the unsubtracted DR for $\Pi^{V,A}(s,m_1,m_2)$ in a way that conforms with the WI, a crucial requirement. We present here an alternative discussion that clarifies some aspects of the derivation. We consider a closed contour in the complex-s plane constructed from straight lines just above and below the real axis from threshold $s = (m_1+m_2)^2$ up to some large cutoff scale $s = \Lambda^2$ and a large circle of radius $|s| = \Lambda^2$. It is understood that this contour is to be described anticlockwise. Application of Cauchy's theorem, Schwartz's reflection principle, and the usual analytic properties derived from perturbation theory leads to

$$\lambda^{V,A}(s,m_1,m_2) = \frac{1}{\pi}\int_{(m_1+m_2)^2}^{\Lambda^2} ds' \frac{\mathrm{Im}\lambda^{V,A}(s',m_1,m_2)}{s'-s-i\epsilon} + \frac{1}{2\pi i}\oint_{|s'|=\Lambda^2} ds' \frac{\lambda^{V,A}(s',m_1,m_2)}{s'} \ , \tag{2.3a}$$

$$\Delta^{V,A}(s,m_1,m_2) = \frac{1}{\pi}\int_{(m_1+m_2)^2}^{\Lambda^2} ds' \frac{\mathrm{Im}\Delta^{V,A}(s',m_1,m_2)}{s'-s-i\epsilon} + \frac{1}{2\pi i}\oint_{|s'|=\Lambda^2} ds' \frac{\Delta^{V,A}(s',m_1,m_2)}{s'} \ , \tag{2.3b}$$

where the cutoff is assumed to satisfy $\Lambda^2 \gg s, m_1^2, m_2^2$. In the integrals over the large circle we have neglected s in the denominators because $\lambda^{V,A}(s',m_1,m_2)$ and $\Delta^{V,A}(s',m_1,m_2)$ are known to behave as constants (modulo logarithms) as $|s'| \to \infty$. Inserting Eq. (2.3) in Eq. (2.2a) and using again this equation to relate the imaginary parts, one obtains

$$\Pi^{V,A}(s,m_1,m_2)=\frac{1}{\pi}\int_{(m_1+m_2)^2}^{\Lambda^2}ds'\left[\frac{\mathrm{Im}\Pi^{V,A}(s',m_1,m_2)}{s'-s-i\epsilon}+\mathrm{Im}\lambda^{V,A}(s',m_1,m_2)\right]+\frac{1}{2\pi i}\oint_{|s'|=\Lambda^2}ds'\frac{\Delta^{V,A}(s',m_1,m_2)-s\lambda^{V,A}(s',m_1,m_2)}{s'}\ . \tag{2.4}$$

The contribution of $\mathrm{Im}\lambda^{V,A}(s',m_1,m_2)$ cancels the quadratic divergence of the first integral. There remains a logarithmic divergence that is regularized by Λ^2. Except for the integrals over the large circle, Eq. (2.4) is the DR proposed in Ref. [20]. As in that paper, we restrict ourselves to the two cases of greatest interest, namely, $m_1=m_2$ and $m_2=0$, which to a very good approximation can be applied to the *tb* isodoublet.

Expanding $\Pi^{V,A}=\Pi_0^{V,A}+(\alpha_s/\pi)\Pi_1^{V,A}+\cdots$ and similarly for $\lambda^{V,A}$ and $\Delta^{V,A}$, calculating the imaginary parts of the one- and two-loop diagrams with constant α_s, and performing the integrations, one finds

$$\Pi_i^V(s,m,m)=\frac{s}{4\pi^2}X_i+\frac{m^2}{\pi^2}V_i(r)-\frac{s}{2\pi i}\oint_{|s'|=\Lambda^2}ds'\frac{\lambda_i^V(s',m,m)}{s'}\ , \tag{2.5a}$$

$$\Pi_i^A(s,m,m)=\frac{s}{4\pi^2}X_i+\frac{m^2}{\pi^2}[Y_i+A_i(r)]+\frac{1}{2\pi i}\oint_{|s'|=\Lambda^2}ds'\frac{\Delta_i^A(s',m,m)-s\lambda_i^A(s',m,m)}{s'}\ , \tag{2.5b}$$

$$\Pi_i^{V,A}(s,m,0)=\frac{s}{4\pi^2}X_i+\frac{m^2}{\pi^2}\left[\frac{Y_i}{4}+F_i(x)\right]+\frac{1}{2\pi i}\oint_{|s'|=\Lambda^2}ds'\frac{\Delta_i^{V,A}(s',m,0)-s\lambda_i^{V,A}(s',m,0)}{s'}\ , \tag{2.5c}$$

where $i=0,1$ labels the one- and two-loop amplitudes, X_i and Y_i are Λ^2-dependent constants, and $V_i(r)$, $A_i(r)$, and $F_i(x)$ are finite functions. Specifically, we have

$$V_0(r)=1-(2r+1)g(r)\ , \tag{2.6a}$$

$$A_0(r)=1-2(r-1)g(r)\ , \tag{2.6b}$$

$$F_0(x)=\frac{1}{2}-\frac{1}{8x}-\frac{1}{4}\left[x+\frac{1}{2}\right]\left[1-\frac{1}{x}\right]^2\times[\ln|1-x|-i\pi\theta(x-1)]\ , \tag{2.6c}$$

where $r=s/4m^2, x=s/m^2$. We have included the color factor, and, defining $D\equiv 1/r-1$,

$$g(r)=\begin{cases}\dfrac{\sqrt{-D}}{2}\left[\ln\dfrac{1+\sqrt{-D}}{|1-\sqrt{-D}|}-i\pi\theta(r-1)\right], & D<0\ ,\\ \sqrt{D}\ \arctan\dfrac{1}{\sqrt{D}}, & D>0\ .\end{cases} \tag{2.6d}$$

The two-loop functions $V_1(r)$, $A_1(r)$, and $F_1(x)$ are studied in detail in Ref. [3]. They depend sensitively on the precise definition of m_t. In Ref. [3], as in most current discussions of electroweak physics, m_t is identified with the zero of the real part of the inverse top-quark propagator. In the literature, it is variously referred to as the *physical, on-shell,* or *dressed* mass. It is also the mass that appears naturally in the application of Cutkosky's rule and the parameter that governs the start of the $t\bar{t}$ cut on the complex-s plane in S-matrix theory. Throughout this paper we follow the same definition. Calling $L=\ln(\Lambda^2/m^2)$, the divergent constants are [20]

$$X_0=X_1=-\tfrac{2}{3}Y_0=L\ , \tag{2.7a}$$

$$Y_1=\tfrac{3}{2}L^2-\tfrac{9}{2}L-1\ . \tag{2.7b}$$

We recall that $\Pi_i^V(s,m,0)=\Pi_i^A(s,m,0)$, with analogous equalities for the λ_i's and Δ_i's.

When, instead of using DR's, the vacuum-polarization functions are evaluated directly in the framework of dimensional regularization one finds [16]

$$\Pi_i^V(s,m,m)=\frac{s}{4\pi^2}\tilde{X}_i+\frac{m^2}{\pi^2}V_i(r)\ , \tag{2.8a}$$

$$\Pi_i^A(s,m,m)=\frac{s}{4\pi^2}\tilde{X}_i+\frac{m^2}{\pi^2}[\tilde{Y}_i+A_i(r)]\ , \tag{2.8b}$$

$$\Pi_i^{V,A}(s,m,0)=\frac{s}{4\pi^2}\tilde{X}_i+\frac{m^2}{\pi^2}\left[\frac{\tilde{Y}_i}{4}+F_i(x)\right]\ . \tag{2.8c}$$

The divergent constants $\tilde{X}_i$ and $\tilde{Y}_i$ are now expressed in terms of $(n-4)$ poles and the 't Hooft mass μ. Specifically,

$$\tilde{X}_0=\frac{1}{\varepsilon}-l+\frac{5}{3}\ , \tag{2.9a}$$

$$\tilde{Y}_0=-\frac{3}{2\varepsilon}+\frac{3}{2}l-3\ , \tag{2.9b}$$

$$\tilde{X}_1=\frac{1}{2\varepsilon}-l-4\zeta(3)+\frac{55}{12}\ , \tag{2.9c}$$

$$\tilde{Y}_1=\frac{3}{2\varepsilon^2}+\frac{1}{\varepsilon}\left[-3l+\frac{11}{4}\right]+3l^2-\frac{11}{2}l+6\zeta(3)+3\zeta(2)-\frac{11}{8}\ , \tag{2.9d}$$

where $\varepsilon=2-n/2$ and $l=\gamma_E+\ln(m^2/4\pi\mu^2)$.

As pointed out in Ref. [20], in the evaluation of physical quantities such as $\Delta\rho$ or Δr the divergent constants X_i, Y_i and, equivalently, $\tilde{X}_i, \tilde{Y}_i$ cancel identically among themselves. In order that Eq. (2.5) be consistent with dimensional regularization, it is clearly necessary that the integrals over the large circle be absorbable in

redefinitions of X_i and Y_i. Moreover, comparison of Eqs. (2.5) and (2.8) shows that, if the integrals are evaluated in dimensional regularization, their effect must be simply to replace X_i and Y_i in the first set of equations by $\tilde{X}_i$ and $\tilde{Y}_i$, respectively. We have verified this by a direct evaluation. We note that the integrals over the large circle receive contributions only from the leading asymptotic terms of the λ_i's and Δ_i's as $|s'|\to\infty$; i.e., terms of $O(1/s')$ do not contribute. One readily finds that the leading asymptotic behaviors of the λ_i's are independent of m_1 and m_2 and of whether we are dealing with vector or axial-vector currents. Furthermore, one verifies that

$$\oint_{|s'|=\Lambda^2} ds' \frac{\Delta_i^{V,A}(s',m,0)}{s'} = \frac{1}{4}\oint_{|s'|=\Lambda^2} ds' \frac{\Delta_i^{A}(s',m,m)}{s'} . \tag{2.10}$$

These results imply that the integrals over the large circle in Eq. (2.5), when evaluated in dimensional regularization, are indeed absorbable in redefinitions of X_i and Y_i. Moreover, the calculation confirms that their effect is to simply replace X_i and Y_i by $\tilde{X}_i$ and $\tilde{Y}_i$, respectively. In particular, for the three cases of greatest interest, Eq. (2.4) leads to

$$\Pi_i^V(s,m,m)=\frac{s}{4\pi^2}(\tilde{X}_i-X_i)+\frac{s}{\pi}\int_{4m^2}^{\Lambda^2}\frac{ds'}{s'}\frac{\mathrm{Im}\Pi_i^V(s',m,m)}{s'-s-i\epsilon} , \tag{2.11a}$$

$$\Pi_i^A(s,m,m)=\frac{s}{4\pi^2}(\tilde{X}_i-X_i)+\frac{m^2}{\pi^2}(\tilde{Y}_i-Y_i) +\frac{1}{\pi}\int_{4m^2}^{\Lambda^2}ds'\left[\frac{\mathrm{Im}\Pi_i^A(s',m,m)}{s'-s-i\epsilon} +\mathrm{Im}\lambda_i^A(s',m,m)\right] , \tag{2.11b}$$

$$\Pi_i^{V,A}(s,m,0)=\frac{s}{4\pi^2}(\tilde{X}_i-X_i)+\frac{m^2}{4\pi^2}(\tilde{Y}_i-Y_i) +\frac{1}{\pi}\int_{m^2}^{\Lambda^2}ds'\left[\frac{\mathrm{Im}\Pi_i^{V,A}(s',m,0)}{s'-s-i\epsilon} +\mathrm{Im}\lambda_i^{V,A}(s',m,0)\right] . \tag{2.11c}$$

In Eq. (2.11a) we have made use of the fact that $\lambda_i^V(s,m,m)=-\Pi_i^V(s,m,m)/s$, which is a consequence of the WI. In Eq. (2.11) the first-degree polynomials in s involving $\tilde{X}_i-X_i$ and $\tilde{Y}_i-Y_i$ cancel the Λ^2 dependence of the integrals and introduce the pole and l contributions of dimensional regularization. Thus, these expressions are suitable for calculations in both modified minimal subtraction ($\overline{\mathrm{MS}}$) and on-shell frameworks.

The DR approach is a very convenient way of performing higher-order calculations and provides a welcome check on the structure of $V_i(r)$, $A_i(r)$, and $F_i(x)$. On the other hand, for the evaluation of $\tilde{X}_i$ and $\tilde{Y}_i$, which are indispensable in the $\overline{\mathrm{MS}}$ scheme, there is no substitute for the dimensional-regularization calculation of Ref. [16]. One could argue that the DR of Eq. (2.4) can be used to evaluate physical observables such as $\Delta\rho$ and Δr. That also has a caveat: indeed, one must show that the integrals over the large circle are absorbable in redefinitions of X_i and Y_i, so that they cancel in these observables. We were able to do this in the case of Eq. (2.5), but only after appealing to the dimensional-regularization evaluation. As explained in the next section, one of the interesting applications of Eq. (2.4) is that, coupled to some very plausible assumptions regarding asymptotic behavior, they provide a framework to analyze $t\bar{t}$ threshold effects that are not taken into account in the usual perturbative calculation.

We close this section with a related topic of general interest, namely, the expression of physical observables such as $\Delta\rho$ and Δr in terms of convergent dispersion integrals. Such *observable radiative corrections* have the property that they are automatically finite, i.e., devoid of $(n-4)$ poles when evaluated in the on-shell renormalization scheme. But this implies that when Eq. (2.4) is substituted into the theoretical expressions for observable radiative corrections, the combination of dispersion integrals that appears must necessarily be convergent as $\Lambda^2\to\infty$. In fact, the cancellation of the $\tilde{X}_i$ and $\tilde{Y}_i$ terms implies that of the X_i and Y_i terms. As X_i and Y_i exactly compensate the Λ^2-dependent terms in the dispersion integrals, this means that the latter also cancel.

The case of $\Delta\rho$ is of sufficient simplicity and interest that it is instructive to give an *ab initio* derivation. Defining ρ as the ratio of the effective coupling strengths of the neutral- and charged-current amplitudes at zero momentum transfer and writing $\rho=1/(1-\Delta\rho)$, the fermionic contribution to $\Delta\rho$ is given by [19,21]

$$\Delta\rho=\frac{A_{WW}^{(f)}(0)}{M_W^2}-\frac{A_{ZZ}^{(f)}(0)}{M_Z^2} , \tag{2.12a}$$

where the A's are the appropriate transverse self-energies, as defined in Ref. [21]. Recalling that $\Pi^V(0,m,m)=0$, the contribution to Eq. (2.12a) due to an isodoublet (1,2) reads

$$(\Delta\rho)_{\mathrm{id}}=\frac{G_F}{\sqrt{2}}\left[\frac{\Pi^A(0,m_1,m_1)+\Pi^A(0,m_2,m_2)}{2} -\Pi^V(0,m_1,m_2)-\Pi^A(0,m_1,m_2)\right] . \tag{2.12b}$$

The WI of Eq. (2.2a) tells us that this can be written in the equivalent form

$$(\Delta\rho)_{\mathrm{id}}=\frac{G_F}{\sqrt{2}}\left[\frac{\Delta^A(0,m_1,m_1)+\Delta^A(0,m_2,m_2)}{2} -\Delta^V(0,m_1,m_2)-\Delta^A(0,m_1,m_2)\right] . \tag{2.12c}$$

Consider now the function

$$f(s,m_1,m_2)=\frac{\Delta^A(s,m_1,m_1)+\Delta^A(s,m_2,m_2)}{2}-\Delta^V(s,m_1,m_2)-\Delta^A(s,m_1,m_2)\ . \quad (2.12d)$$

As Eq. (2.12c) is finite and the divergences in $\Delta^{V,A}(s,m_1,m_2)$ are independent of s, we see that Eq. (2.12d) is finite for all values of s. [Here *finite* means free of $(n-4)$ poles.] Moreover, we expect that

$$\lim_{\Lambda^2\to\infty}\oint_{|s'|=\Lambda^2}\frac{ds'}{s'}f(s',m_1,m_2)=0\ , \quad (2.12e)$$

so that $f(s,m_1,m_2)$ obeys an unsubtracted DR,

$$f(s,m_1,m_2)=\frac{1}{\pi}\int_{(m_1+m_2)^2}^{\infty}ds'\frac{\mathrm{Im}f(s',m_1,m_2)}{s'-s-i\epsilon}\ . \quad (2.12f)$$

We have explicitly verified Eq. (2.12e) for arbitrary m_1 and m_2 at one loop and for $m_2=0$ at two loops, in which case it reduces to Eq. (2.10). We conclude that $(\Delta\rho)_{\mathrm{id}}$ can be expressed succinctly as a convergent dispersion integral:

$$(\Delta\rho)_{\mathrm{id}}=\frac{G_F}{\sqrt{2}}f(0,m_1,m_2)=\frac{G_F}{\pi\sqrt{2}}\int_{(m_1+m_2)^2}^{\infty}\frac{ds'}{s'}\mathrm{Im}f(s',m_1,m_2)\ . \quad (2.12g)$$

For the purposes of this paper the most interesting application of Eq. (2.12g) is to analyze the tb contribution to $\Delta\rho$. Approximating $m_b=0$ and recalling that $\Delta_i^V(s,m,0)=\Delta_i^A(s,m,0)$ and $\Delta_i^A(s,0,0)=0$ $(i=0,1)$, Eqs. (2.12d) and (2.12g) lead to

$$(\Delta\rho)_{tb}=\frac{G_F}{\pi\sqrt{2}}\int_{m_t^2}^{\infty}\frac{ds'}{s'}\mathrm{Im}\left[\frac{\Delta^A(s',m_t,m_t)}{2}-2\Delta^A(s',m_t,0)\right]\ . \quad (2.13)$$

As we shall see below, this simple integral representation will permit us to understand almost immediately why the threshold effects associated with the $t\bar{t}$ and $t\bar{b}$ channels give a contribution to $\Delta\rho$ of the same sign as the perturbative $O(\alpha\alpha_s)$ terms. We also note that Eq. (2.13) can directly be obtained by setting $m_2=0$ and inserting Eqs. (2.11b) and (2.11c) into Eq. (2.12b). As the $\Delta^{V,A}(s,m_1,m_2)$ functions involve the divergence of the vector and axial-vector currents, we recover from Eqs. (2.12d), (2.12g), and (2.13) the notion that $\Delta\rho$ is a measure of weak-isospin breaking.

III. INCORPORATION OF THRESHOLD EFFECTS

Threshold effects involving the $t\bar{t}$, $t\bar{b}$, and $b\bar{b}$ channels can be expressed as contributions to $\mathrm{Im}\Pi^{V,A}(s,m_1,m_2)$ [12,13] and $\mathrm{Im}\lambda^{V,A}(s,m_1,m_2)$. In the following, our aim is to analyze how they affect $\Pi^{V,A}(s,m_1,m_2)$, and we propose to do so on the basis of Eq. (2.4). In using the DR approach we assume that the threshold effects do not alter the leading high-$|s|$ behaviors of $\lambda_i^{V,A}(s,m_1,m_2)$ and $\Delta_i^{V,A}(s,m_1,m_2)$, so that the integrals over the large circle are not affected. This is equivalent to assuming that the leading asymptotic behaviors of $\lambda_i^{V,A}(s,m_1,m_2)$ and $\Delta_i^{V,A}(s,m_1,m_2)$ are given by the usual perturbative results discussed in the previous section, with the threshold effects providing only subleading contributions that vanish as $|s|\to\infty$. In particular, $f(s,m_t,0)$ still satisfies an unsubtracted DR and $(\Delta\rho)_{tb}$ can still be expressed in terms of the dispersion integral of Eq. (2.13). As the threshold effects on the imaginary parts have support over a small, bounded range, the corresponding contributions to the dispersion integrals are rapidly convergent and the resulting functions vanish as $|s|\to\infty$. Thus, the above assumption is very plausible and self-consistent. In summary, in our formulation threshold effects are described by the DR's [20]

$$\Pi^{V,A}(s,m_1,m_2)=\frac{1}{\pi}\int ds'\left[\frac{\mathrm{Im}\Pi^{V,A}(s',m_1,m_2)}{s'-s-i\epsilon}+\mathrm{Im}\lambda^{V,A}(s',m_1,m_2)\right]\ , \quad (3.1a)$$

where the range of integration is to be chosen such that the threshold support, which starts below the open-flavor threshold, is included.

Using Eq. (2.2a), we see that $\Pi^{V,A}(s,m_1,m_2)$ can alternatively be written as

$$\Pi^{V,A}(s,m_1,m_2)=\frac{s}{\pi}\int\frac{ds'}{s'}\frac{\mathrm{Im}\Pi^{V,A}(s',m_1,m_2)}{s'-s-i\epsilon}+\frac{1}{\pi}\int\frac{ds'}{s'}\mathrm{Im}\Delta^{V,A}(s',m_1,m_2)\ . \quad (3.1b)$$

We note that this representation can be directly derived from the following assumptions: (i) $\Pi^{V,A}(s,m_1,m_2)$ satisfies a once-subtracted DR; (ii) the subtraction constant is determined from the WI of Eq. (2.2a), so that $\Pi^{V,A}(0,m_1,m_2)=\Delta^{V,A}(0,m_1,m_2)$; and (iii) $\Delta^{V,A}(s,m_1,m_2)$ satisfies an unsubtracted DR, so that $\Delta^{V,A}(0,m_1,m_2)$ can be calculated from the second integral of Eq. (3.1b). Thus, the DR's for $\Pi^{V,A}(s,m_1,m_2)$ proposed in Ref. [20] to study threshold effects, namely, Eqs. (3.1a) or (3.1b), are the simplest possible ones consistent with the WI of Eq. (2.2a). The latter is, of course, a crucial requirement.

It is important to note that, according to Eq. (3.1), threshold effects modify the asymptotic behavior of $\Pi^{V,A}(s,m_1,m_2)$ as $|s|\to\infty$ by constant terms, i.e., subleading contributions. Therefore, considerable care must be exercised in attempting to evaluate these effects by considering unsubtracted DR's for combinations of $\Pi^{V,A}$ functions, judiciously chosen so that the usual perturbative contributions vanish as $|s|\to\infty$. Indeed, when threshold effects are incorporated, it is possible that such combinations do not vanish as $|s|\to\infty$, in which case the assumption of unsubtracted DR's is no longer warranted.

In the remainder of this paper, we shall focus on the $t\bar{t}$ threshold. Threshold effects associated with the $t\bar{b}$ chan-

nel are known to be proportional to the square of the reduced mass of the $t\bar{b}$ system [13] and can be neglected.[1] This suppression also manifests itself in the fact that close to threshold the continuum results for $\mathrm{Im}\Pi_l^{V,A}(s,m,0)$ and $\mathrm{Im}\lambda_l^{V,A}(s,m,0)$ scale like v^2, where $v=(s-m^2)/(s+m^2)$ is the velocity of the massive quark in the center-of-mass system (c.m.s.) [20]. Threshold effects in the $b\bar{b}$ channel, i.e., bottonium resonances, give significant contributions only to the photon self-energy, which are routinely included [6]. Thus, only the case $m_1=m_2=m_t$ is relevant in our applications.

We conclude this section by collecting the DR's on which our subsequent analysis will be based. They read

$$\Pi^V(s,m_t,m_t)=\frac{s}{\pi}\int\frac{ds'}{s'}\frac{\mathrm{Im}\Pi^V(s',m_t,m_t)}{s'-s-i\epsilon}\,, \tag{3.2a}$$

$$\Pi^A(s,m_t,m_t)=\frac{1}{\pi}\int ds'\left[\frac{\mathrm{Im}\Pi^A(s',m_t,m_t)}{s'-s-i\epsilon}+\mathrm{Im}\lambda^A(s',m_t,m_t)\right]. \tag{3.2b}$$

While threshold effects on $\mathrm{Im}\Pi^V(s,m_t,m_t)$ are well understood [12,13], $\mathrm{Im}\Pi^A(s,m_t,m_t)$ and $\mathrm{Im}\lambda^A(s,m_t,m_t)$ seem, at first sight, to require a separate analysis. In the next section we shall see that this task is greatly facilitated by the fact that at threshold the $t\bar{t}$ system is essentially nonrelativistic.

IV. PARAMETRIZATION OF THE $t\bar{t}$ THRESHOLD

As pointed out in the Introduction, the shape of the $t\bar{t}$ threshold is expected to depend crucially on the value of m_t. For m_t close to its lower bound there should be a rich spectrum of distinct nonrelativistic states bound by strong long-range forces. For increasing m_t, however, the weak decay of a single top quark inside the bound states comes to dominate their widths. At $m_t\approx 130$ GeV the widths surpass the $1S$-$2S$ mass difference, so that the bound-state resonances lose their separate identities and smear together into a broad threshold enhancement. Although it is then still technically possible to compute the characteristic parameters of the individual resonances, their physical interpretation becomes dubious, and it appears more reliable to directly calculate the imaginary part of the Green's function of the Schrödinger equation that characterizes the $t\bar{t}$ system allowing for a complex energy. The latter formulation effectively resums the contributions of soft multigluon exchanges in the ladder approximation. In our analysis we shall adopt the resonance parametrization of Ref. [13] in the lower-m_t range and the Green's function approach of Ref. [12], although in a slightly modified form, in the upper-m_t range. Prior to discussing these two methods, we shall briefly review the perturbative results up to $O(\alpha\alpha_s)$, which have to be subtracted in order to avoid double counting.

Within perturbation theory, the imaginary parts that enter Eq. (3.2) exhibit the following threshold behaviors:

$$\frac{1}{s}\mathrm{Im}\Pi^V(s,m_t,m_t)=\frac{N_c}{12\pi}\frac{v}{2}(3-v^2)\left[1+C_F\frac{\alpha_s}{\pi}\left[\frac{\pi^2}{2v}-4+O(v)\right]+\cdots\right], \tag{4.1a}$$

$$\frac{1}{s}\mathrm{Im}\Pi^A(s,m_t,m_t)=\frac{N_c}{12\pi}v^3\left[1+C_F\frac{\alpha_s}{\pi}\left[\frac{\pi^2}{2v}-2+O(v)\right]+\cdots\right], \tag{4.1b}$$

$$-\mathrm{Im}\lambda^A(s,m_t,m_t)=\frac{N_c}{12\pi}\frac{v}{2}(3-v^2)\left[1+C_F\frac{\alpha_s}{\pi}\left[\frac{\pi^2}{2v}-3+O(v)\right]+\cdots\right], \tag{4.1c}$$

where $N_c=3$, $C_F=(N_c^2-1)/2N_c$, and $v=\sqrt{1-4m_t^2/s}$ is the velocity of either quark in the c.m.s. Full expressions for the $O(\alpha_s)$ terms may be found in Refs. [3,20]. We notice that $\mathrm{Im}\Pi^A(s,m_t,m_t)$ is suppressed near threshold by two powers of v relative to $\mathrm{Im}\Pi^V(s,m_t,m_t)$. This may be understood by observing that $\mathrm{Im}\Pi^V(s,m_t,m_t)$ corresponds to kinematically preferred $J^P=1^-$ states, with $L=0$, while $\mathrm{Im}\Pi^A(s,m_t,m_t)$ couples to 1^+ states, with $L=1$, which are disfavored due to centrifugal barrier effects. On the other hand, $\mathrm{Im}\lambda^A(s,m_t,m_t)$ receives contributions also from 0^- states, with $L=0$, which are again not subject to suppression. In fact, $\mathrm{Im}\lambda^A(s,m_t,m_t)\approx-\mathrm{Im}\Pi^V(s,m_t,m_t)/s$ holds true in the nonrelativistic regime. We shall see below that this relation can be explicitly verified in both resonance and Green's function approaches. We note further that for $v\to 0$ the $O(\alpha_s)$ corrections of Eq. (4.1) are enhanced relative to the lowest-order results by the universal term $\pi C_F\alpha_s/2v$, which is the QCD analogue of Sommerfeld's Coulomb rescattering correction [22]. In the framework of nonrelativistic quantum mechanics, this term is absorbed in the wave functions of the bound states. The leading relativistic corrections to this term are attributed to the exchange of a virtual hard gluon between the quarks and will be implemented explicitly in the nonrelativistic formalism to refine the prediction.

We now make some observations concerning the renormalization scale μ of α_s in self-energy contributions induced by the tb doublet. Since present knowledge reaches only to leading order in QCD, conventional methods of optimizing μ such as the concept of fastest apparent convergence [23] or the principle of minimal sensitivity [24] cannot be applied. However, the mean-value theorem of integration provides a consistent procedure to fix μ within the dispersive formalism. Toward

[1]The occurrence of a Coulomb singularity in $\Pi_1^V(s,m_t,m_b)$ at $s=M_W^2$ is excluded because $M_W^2<(m_t+m_b)^2$.

this end, one calculates the tb contribution to some electroweak observable in two different ways, namely, once with μ linked to the integration variable s' and once with μ kept fixed, and equates the two results. The matching point comes out typically in the vicinity of $\mu=m_t$. This choice can be motivated independently by direct inspection of the two-loop amplitudes [25] and by arguments based on an effective field theory [26]. By this means, it is, of course, difficult to reliably distinguish between $\mu=m_t/2$ and $\mu=2m_t$, say, and there remains a theoretical uncertainty which may be regarded as being of $O(\alpha_s^2)$ and higher. We stress that all these considerations ignore $t\bar{t}$ threshold effects that arise from the resummation of the perturbation series—or are of a nonperturbative nature.

In the resonance picture, $\mathrm{Im}\Pi^V(s,m_t,m_t)$ can be approximated by a series of δ functions [13]:

$$\frac{1}{s}\mathrm{Im}\Pi^V(s,m_t,m_t)=\sum_n N_c\left[1-4C_F\frac{\alpha_s(M_n)}{\pi}\right]\times\frac{|R_n(0)|^2}{M_n}\delta(s-M_n^2)\ , \tag{4.2a}$$

where M_n and $R_n(0)$ are the mass and the radial wave function at the origin of the nth excited state, respectively, and the QCD correction factor may be gleaned from Eq. (4.1a). The interactions between the quarks are described by a nonrelativistic, and thus spin-independent, QCD potential. The positions and strengths of the resonances are, therefore, determined by the radial equation of motion and controlled by the angular momentum quantum number L. Consequently, the dominant contributions to $\mathrm{Im}\lambda^V(s,m_t,m_t)=-\mathrm{Im}\Pi^V(s,m_t,m_t)/s$ and $\mathrm{Im}\lambda^A(s,m_t,m_t)$ are characterized by the same values of M_n and $R_n(0)$. Adjusting the QCD factor according to Eq. (4.1c), we find that

$$-\mathrm{Im}\lambda^A(s,m_t,m_t)=\sum_n N_c\left[1-3C_F\frac{\alpha_s(M_n)}{\pi}\right]\times\frac{|R_n(0)|^2}{M_n}\delta(s-M_n^2)\ . \tag{4.2b}$$

From the above discussion it is obvious that we may safely neglect $\mathrm{Im}\Pi^A(s,m_t,m_t)$ in the threshold region.

In our analysis we use the values of M_n and $|R_n(0)|$ which have been calculated in Ref. [13] for the twelve lowest-lying toponium states as a function of m_t in the nonrelativistic quark model endowed with the Richardson potential [27]. To ameliorate the matching between the resonance and continuum parametrizations, we adopt the local-duality recipe suggested in Ref. [28] and choose $\mu=2|\mathbf{p}|=\sqrt{s-4m_t^2}$ in the perturbative result, where $\mathbf{p}$ is the three-momentum of either quark in the c.m.s. We do this in the range $(2m_T)^2\le s\le 5m_t^2$, where $m_T=m_t+400$ MeV roughly represents the mass of the $t\bar{u}$ or $t\bar{d}$ mesons T. In this way, $\alpha_s(\mu)$ increases towards the threshold, simulating the onset of confinement. (We note that throughout this transition region μ takes a value that corresponds to five active quark flavors.) The upper end of the interval is chosen so that at this point $\mu=m_t$, the scale advocated for the purely perturbative treatment of tb contributions. Thus, at $s=5m_t^2$ the two evaluations of the imaginary parts, with $\mu=2|\mathbf{p}|$ and constant $\mu=m_t$, merge. For $s\ge 5m_t^2$, the imaginary parts are identified with the usual perturbative contributions evaluated with $\alpha_s(m_t)$. To determine the excess threshold effect relative to the usual perturbative calculation, we subtract the contribution to Eq. (3.2) coming from the latter, evaluated with $\alpha_s(m_t)$ and integrated along the interval $4m_t^2\le s\le 5m_t^2$.

In the Green's function approach, $\mathrm{Im}\Pi^V(s,m_t,m_t)$ is given by [12]

$$\frac{1}{s}\mathrm{Im}\Pi^V(s,m_t,m_t)=N_c\left[1-4C_F\frac{\alpha_s(2m_t)}{\pi}\right]\frac{1}{2m_t^2}\times\mathrm{Im}G(0,0;\sqrt{s}-2m_t+i\Gamma_t)\ , \tag{4.3a}$$

where $G(\mathbf{r},\mathbf{r}';E+i\Gamma_t)$ is the solution of the nonrelativistic Schrödinger equation of the $t\bar{t}$ system bound by the potential $V(\mathbf{r})$,

$$[H-(E+i\Gamma_t)]G(\mathbf{r},\mathbf{r}';E+i\Gamma_t)=\delta^{(3)}(\mathbf{r}-\mathbf{r}')\ , \tag{4.3b}$$

with the Hamiltonian

$$H=-\frac{1}{m_t}\nabla^2+V(\mathbf{r})\ . \tag{4.3c}$$

Notice that this correctly reflects the reduced mass $m_t/2$ and effective width $2\Gamma_t$ of the particle-antiparticle system. The authors of Ref. [12] considered only vector currents. However, replacing in their Eq. (3.2) the vector couplings by axial-vector ones and repeating, mutatis mutandis, the subsequent analysis, one finds that

$$-\mathrm{Im}\lambda^A(s,m_t,m_t)=N_c\left[1-3C_F\frac{\alpha_s(2m_t)}{\pi}\right]\frac{1}{2m_t^2}\times\mathrm{Im}G(0,0;\sqrt{s}-2m_t+i\Gamma_t)\ , \tag{4.3d}$$

where the QCD factor again follows from Eq. (4.1c), while $\mathrm{Im}\Pi^A(s,m_t,m_t)=0$ as anticipated above.

We deviate from the procedure of Ref. [12] in the following two respects. First, we employ the potential J by Igi and Ono [29], which accurately describes charmonium and bottonium spectroscopy; to be consistent with a recent global QCD analysis [30], we set $\Lambda^{(4)}_{\overline{\mathrm{MS}}}=300$ MeV in that potential. Second, we include QCD corrections to the top-quark decay width Γ_t [31]. We include the contributions of Eq. (4.3) in the range $(2m_t-\sqrt{m_t\Gamma_t})^2\le s\le(2m_t+800\ \mathrm{MeV})^2$. The lower bound ensures that in all cases of interest the binding energy $E=\sqrt{s}-2m_t$ of the $t\bar{t}$ system satisfies $|E|\le\sqrt{m_t\Gamma_t}\ll 2m_t$, consistent with the underlying nonrelativistic approximation, and that the domain where $\mathrm{Im}G(0,0;\sqrt{s}-2m_t+i\Gamma_t)$ contributes significantly is included; cf. Ref. [12]. At $s=(2m_t+800\ \mathrm{MeV})^2$, the Green's function results are already quite close to the usual continuum calculation with $\mu=2|\mathbf{p}|$, so

that from this point onwards we use the same transition method as in the resonance approach. In particular, we have to correct for double counting in the interval $4m_t^2 \le s \le 5m_t^2$ by subtracting, as before, the perturbative results.

Figure 1 compares the three different parametrizations of $\mathrm{Im}\Pi^V(s,m_t,m_t)$ in the threshold region, as a function of E, for selected values of m_t. The dashed curves correspond to the perturbative results up to $O(\alpha\alpha_s)$, with α_s evaluated at the constant $\mu=m_t$, for which the dispersion integral of Eq. (2.11a) can be solved analytically to yield

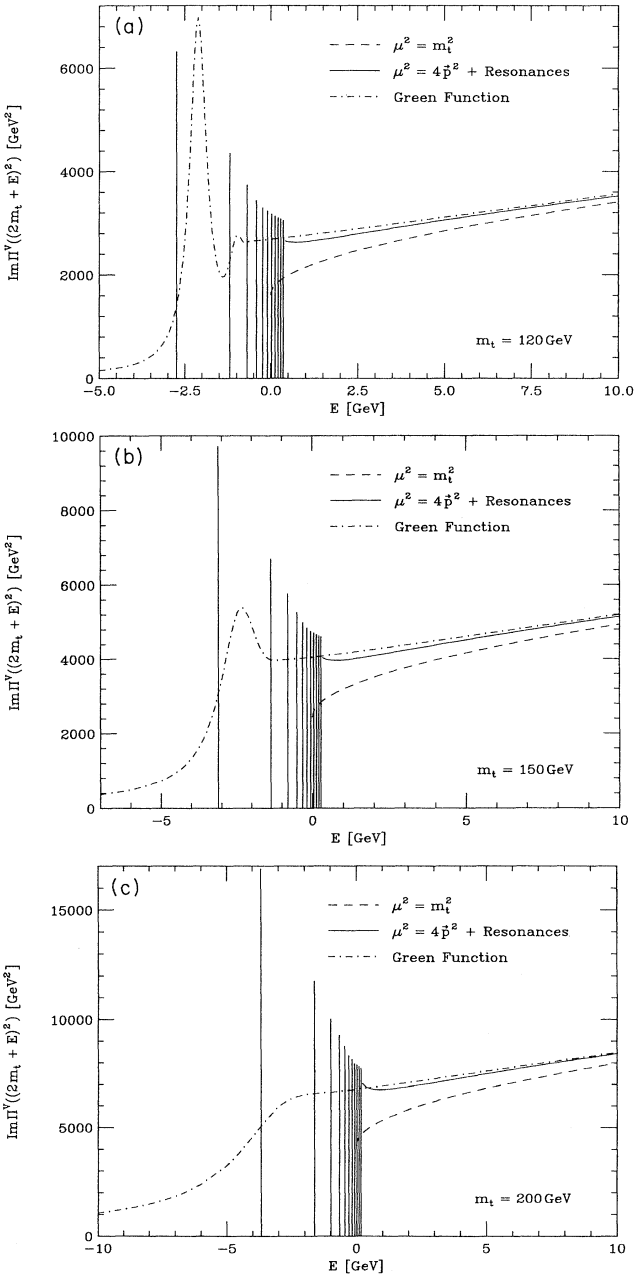

FIG. 1. Perturbative, resonance, and Green's function parametrizations of $\mathrm{Im}\Pi^V(s,m_t,m_t)$ in the threshold region as a function of $E \equiv \sqrt{s} - 2m_t$, assuming (a) $m_t = 120$ GeV, (b) $m_t = 150$ GeV, and (c) $m_t = 200$ GeV; see text.

the familiar expressions [2,3]. The vertical lines visualize the δ functions of Eq. (4.2a). Their heights have been adjusted in such a way that the histogram, which is spanned by connecting their peaks in stepwise fashion starting out from the leftmost one, measures the integral over the δ functions. Specifically, if we integrate $\mathrm{Im}\Pi^V(s,m_t,m_t)$ over E using Eq. (4.2a), the area of the first (leftmost) rectangle in the histogram represents the contribution to this integral of the first (leftmost) resonance, the area of the second rectangle from the left represents the contribution of the second resonance, and so on. The adjacent solid curves represent the continuum results with $\mu=2|\mathbf{p}|$. We point out that these curves would set on somewhat too high if $\mu=|\mathbf{p}|$ was used; for a detailed discussion of this point see also Ref. [11]. Finally, the dot-dashed curves illustrate the Green's function parametrizations by Eq. (4.3a). The Richardson potential has a more singular short-distance behavior than the two-loop potential that we use to compute the Green's functions, so that the $1S$ state is shifted to lower energy relative to the latter case. This reflects the model dependence of our analysis. However, this uncertainty in location is inconsequential after integration. We do not show curves for $\mathrm{Im}\lambda^A(s,m_t,m_t)$ because they exhibit very similar qualitative features.

V. RESULTS

In the following, we shall work in the on-mass-shell scheme [5]. A comprehensive analysis in the $\overline{\mathrm{MS}}$ scheme will be reported on in a forthcoming paper [32]. Before presenting our final quantitative results, we reveal the main qualitative features by drastically simplifying both resonance and Green's function approaches. We first consider a single toponium resonance θ with mass $M_\theta \approx 2m_t$. Neglecting the hard-gluon correction factors, we may write Eq. (4.2) as

$$\frac{1}{s}\mathrm{Im}\Pi^V(s,m_t,m_t) = -\mathrm{Im}\lambda^A(s,m_t,m_t) = \pi f_V^2 M_\theta^2 \delta(s-M_\theta^2)\,, \tag{5.1}$$

where $f_V^2 = N_c|R_\theta(0)|^2/(\pi M_\theta^3)$ is a dimensionless constant measuring the vector coupling strength of θ. The presence of θ induces the following additional contributions in $\Delta\rho$ and Δr:

$$\delta(\Delta\rho) = -\frac{G_F}{2\sqrt{2}} f_V^2 M_\theta^2\,, \tag{5.2a}$$

$$\delta(\Delta r) = -\frac{c_W^2}{s_W^2}\delta(\Delta\rho)\left[1-\left[1-\frac{8}{3}s_W^2\right]^2\frac{M_Z^2}{M_\theta^2-M_Z^2}\right] + \frac{16}{9}\pi\alpha f_V^2\,, \tag{5.2b}$$

where $c_W^2 = 1-s_W^2 = M_W^2/M_Z^2$. Equation (5.2a) follows immediately from Eq. (2.13) using Eqs. (2.2a) and (5.1) and recalling that $\mathrm{Im}\Pi^A(s,m_t,m_t) \approx 0$ near threshold. For phenomenologically acceptable QCD potentials, the empirical relation $|R_n(0)|^2 \propto m_{\mathrm{red}}^2$, where m_{red} denotes the reduced mass of the quark system, is approximately

satisfied for given n [13]. In the case of the Richardson potential, the proportionality factor of the $1S$ state is roughly 1.1 GeV in the $b\bar{b}$ and $t\bar{b}$ channels, and varies between 1.9 and 2.8 GeV for $M_Z \leq m_t \leq 200$ GeV in the $t\bar{t}$ channel [13]. Hence, $-\delta(\Delta\rho)$ increases with m_t, and so does $\delta(\Delta r)$ for $m_t \gg M_Z/2$. Notice the enhancement factor of c_W^2/s_W^2 in Eq. (5.2b).

As anticipated in Sec. II, threshold effects associated with the tb doublet shift $\Delta\rho$ in the same direction as the familiar $O(\alpha\alpha_s)$ corrections. The sign of the effect can also be understood directly from the basic equations (2.1) and (2.2). The contributions of a sharp 0^- toponium resonance to $\lambda^A(s,m_t,m_t)$ and $\Delta^A(s,m_t,m_t)$ are $f_\theta^2/(s-M_\theta^2)$ and $f_\theta^2 M_\theta^2/(s-M_\theta^2)$, respectively, where f_θ is defined by $\langle 0|J_\mu^A(0)|\theta(q)\rangle = if_\theta q_\mu$. The WI of Eq. (2.2a) tells us then that $\Pi^A(s,m_t,m_t)$ receives a corresponding contribution $-f_\theta^2$. Inserting this result into the first term of Eq. (2.12b), with $m_1 = m_t$ and $m_2 = 0$, we find a contribution $-G_F f_\theta^2/2\sqrt{2}$, which is consistent with Eq. (5.2a). A related argument, involving spontaneously broken axial-vector currents, is often invoked to explain the generation of the vector-boson masses in technicolor theories. To stress the similarity, we note that $G_F M_Z^2 f_\theta^2/2\sqrt{2}$ is part of $A_{ZZ}^{(f)}(0)$ in Eq. (2.12a), and can therefore be interpreted as a contribution to the Z-boson mass.

In the Green's function approach, the $t\bar{t}$ excitation curve can be imitated crudely by lowering the open-flavor threshold of the perturbative result from $s = 4m_t^2$ to $s = (2m_t - \Delta)^2$ and by defining in this interval

$$\frac{1}{s}\mathrm{Im}\Pi^V(s,m_t,m_t) = -\mathrm{Im}\lambda^A(s,m_t,m_t) = \frac{N_c C_F}{16}\alpha_s(\mu) , \tag{5.3}$$

which continuously merges into Eqs. (4.1a) and (4.1c). The length and height of this rectangle are controlled by the free parameters Δ and μ, respectively, while m_t is regarded as fixed. Up to terms of $O(\Delta^2)$, the resulting contributions to $\Delta\rho$ and Δr read

$$\delta(\Delta\rho) = -\frac{G_F}{8\sqrt{2}} N_c C_F \frac{\alpha_s(\mu)}{\pi} m_t \Delta , \tag{5.4a}$$

$$\delta(\Delta r) = -\frac{c_W^2}{s_W^2}\delta(\Delta\rho)\left[1 - \left[1 - \frac{8}{3}s_W^2\right]^2 \frac{M_Z^2}{(2m_t)^2 - M_Z^2}\right] + \frac{N_c C_F \alpha\alpha_s(\mu)\Delta}{9m_t} . \tag{5.4b}$$

This exhibits a similar structure as Eq. (5.2), which nicely demonstrates the duality of the two underlying pictures. Taking Δ and μ to be roughly m_t independent, $\Delta\rho$ again receives a negative correction that increases with m_t. The above discussion is only qualitative. The detailed calculations show that, in the range 150 GeV $\leq m_t \leq 250$ GeV, the threshold contributions to $\Delta\rho$ and ΔT increase with m_t faster in the Green's function than in the resonance approach, and that both grow more rapidly than m_t.

Our quantitative analysis of the continuum contributions in $O(\alpha)$ and $O(\alpha\alpha_s)$ is based on Ref. [15] with the modifications suggested in Ref. [33]. We incorporate the result of a very recent calculation [18] of two-loop corrections to the ρ parameter, which generalizes the formula of Ref. [17] to arbitrary Higgs-boson masses M_H. We employ the three-loop formula for $\alpha_s(\mu)$ [34], which we adjust in such a way that $\alpha_s(M_Z) = 0.117$ [30]. We adopt the parametrization of the light-quark sector from Ref. [35]. We use $M_Z = 91.187$ GeV [36] and otherwise employ the standard-model parameters of Ref. [37].

Our final results are presented in Figs. 2–5. Figure 2 demonstrates the significance of QCD corrections for the mass relation established by Δr. Both continuum and

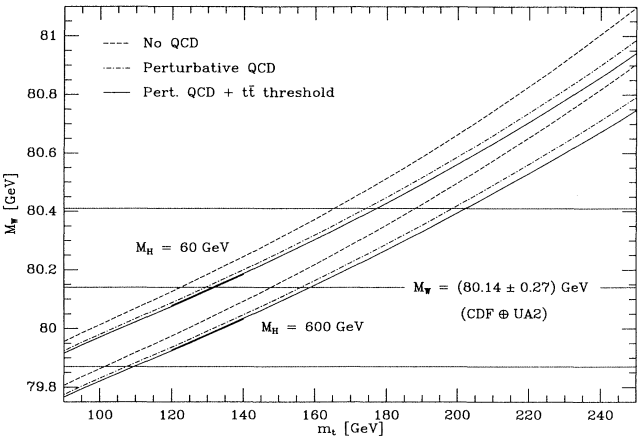

FIG. 2. Predictions of M_W as a function of m_t for $M_H = 60$ GeV and $M_H = 600$ GeV from α, G_F, and M_Z. The dashed lines represent the electroweak calculation with $\alpha_s = 0$, the dot-dashed lines include the perturbative $O(\alpha\alpha_s)$ corrections, and the solid lines include the additional contributions from $t\bar{t}$ threshold effects. The latter are evaluated in the resonance approach for $m_t \leq 140$ GeV and the Green's function formulation for $m_t \geq 120$ GeV; the difference between the two methods in the range 120 GeV $\leq m_t \leq 140$ GeV is not visible in the figure. For comparison, we display the current value of M_W from CDF and UA2 measurements.

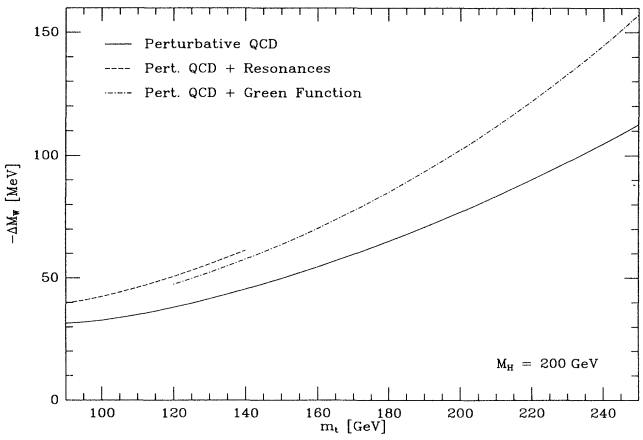

FIG. 3. Shift of M_W due to perturbative QCD corrections (solid line) plus $t\bar{t}$ threshold effects calculated in the resonance approach (dashed line) and the Green's function approach (dot-dashed line) as a function of m_t, assuming $M_H = 200$ GeV.

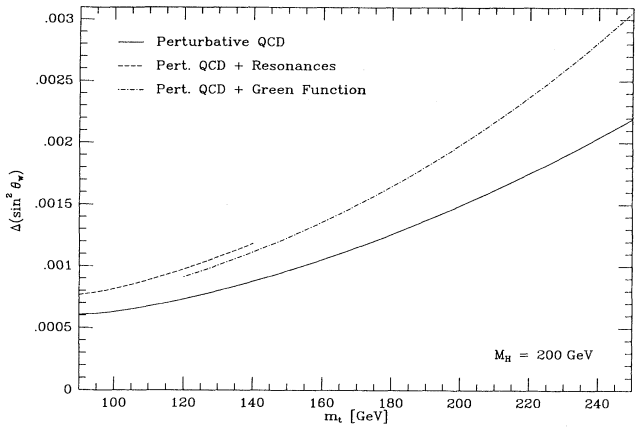

FIG. 4. Shift of $\sin^2\theta_W$, as a function of m_t, assuming $M_H=200$ GeV; see caption of Fig. 3.

threshold contributions act in the same direction, and at high m_t their combined effect becomes comparable in size to the uncertainty caused by the lack of knowledge of M_H. For comparison, also the combined result of the M_W measurement by Collider Detector at Fermilab (CDF) and UA2 Collaborations [38] is shown. It is clear that measurements of m_t to $\sim\pm5$ GeV and of M_W to $\sim\pm50$ GeV would give valuable information about M_H. Figure 3 illustrates, in the case of the M_W shift, the relative size of the threshold effects and the usual $O(\alpha\alpha_s)$ corrections originating from the continuum. We see that, depending on m_t, the former amount to 25–40 % of the latter. Already for $m_t\gtrsim150$ GeV, the overall QCD-induced M_W shift exceeds the expected experimental error of the M_W measurement planned at LEP 2. Figure 4 displays the same information in terms of $\sin^2\theta_W\equiv1-M_W^2/M_Z^2$. Figure 5 shows by how much QCD corrections shift the value of m_t predicted from current M_W measurements. In Figs. 3–5, we have assumed the central value $M_H=200$ GeV. However, the M_H dependence essentially cancels out in the parameter shifts considered there.

At this point, we roughly estimate the errors on the

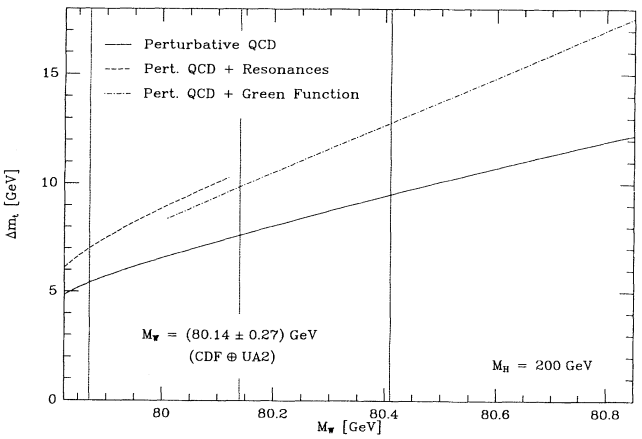

FIG. 5. Shift of m_t, as a function of M_W, assuming $M_H=200$ GeV; see caption of Fig. 3.

evaluation of the M_W shift. Of course, every QCD analysis suffers from the relatively poor knowledge of α_s. The current world average at the Z-boson scale is $\alpha_s(M_Z)=0.117\pm0.007$ [30]. In the continuum, the QCD corrections are proportional to $\alpha_s(\mu)$, so that the experimental error is roughly $\pm6\%$. To estimate the theoretical error, which is mainly due to the lack of knowledge of terms beyond $O(\alpha\alpha_s)$ we vary μ between $m_t/2$ and $2m_t$. This changes $\alpha_s(\mu)$ by typically $\pm10\%$. Moreover, if we recall that the $O(\alpha\alpha_s)$ corrections to $\Delta\rho$ and to the m_t-dependent part of Δr are $\sim10\%$, it appears plausible that terms of $O(\alpha\alpha_s^2)$ may, in fact, amount to $\sim10\%$ of the $O(\alpha\alpha_s)$ contributions. It is clear that knowledge of the tb contributions in $O(\alpha\alpha_s^2)$ is requisite in order to further constrain the fudge factor in the choice of μ. We thus argue that the total error in the continuum calculation is presently at the level of $\pm15\%$. To determine the experimental error on the threshold contributions, we repeat our Green's function analysis using the parametrizations of the J-type Igi-Ono potential appropriate for $\Lambda^{(4)}_{\overline{\rm MS}}=200$ and 400 MeV, which roughly correspond to $\alpha_s(M_Z)=0.110$ and 0.124, respectively. We find a variation of $\pm16\%$, which is nearly three times as large as the experimental error in the continuum. This may be understood by observing that the line shape of the $1S$ resonance is highly sensitive to α_s, the dependence of the peak height on α_s being approximately cubic for $m_t\lesssim150$ GeV [12]. Furthermore, the prediction of the $t\bar{t}$ excitation curve depends to some extent on the underlying quark-model assumptions. To estimate this model dependence, we have compared the resonance approach, with the Richardson potential, and the Green's function approach, with the Igi-Ono potential, in the transition region $120\le m_t\le140$ GeV. We have also checked that the potential used in Ref. [12] yields results that are rather close to those based on the Igi-Ono potential. This leads us to an estimated theoretical error of $\pm15\%$ on the threshold effects. Thus, the total error in the threshold calculation is at the level of $\pm30\%$. Taking into account that, for $M_Z\le m_t\le250$ GeV, the threshold contributions make up 20–30 % of the total QCD corrections, we conclude that our overall QCD predictions have an error of $\sim\pm20\%$. Finally, it is encouraging to point out that, although one expects the resonance and Green's function approaches to be preferable at lower and higher m_t values, respectively, the M_W shifts predicted by the two methods are, in fact, rather close over the entire range $M_Z\le m_t\le250$ GeV [32].

VI. CONCLUSIONS

We have investigated the sensitivity of central electroweak quantities such as $\Delta\rho$ and Δr to the precise shape of the $t\bar{t}$ excitation curve in e^+e^- annihilation. For $m_t\lesssim130$ GeV, we have parametrized the threshold line shape by a spectrum of separate toponium resonances along with a suitably adjusted continuum onset [11,13,28]. For higher values of m_t, we have employed a Green's function technique which automatically resums to leading-logarithmic order in QCD the ladder diagrams

involving the exchange of any number of uncrossed gluons [10,12]. By the optical theorem, $\sigma(e^+e^-\to t\bar{t})$ corresponds to the absorptive parts of the photon and Z-boson self-energies, and its enhancement at threshold induces additional contributions in the corresponding real parts, which are not included in the usual perturbative calculations to $O(\alpha\alpha_s)$. We have evaluated these contributions by means of dispersion relations which manifestly satisfy the underlying Ward identities [20] and have analyzed the resulting shifts in $\Delta\rho$ and Δr. The threshold effects turn out to reduce the value of M_W predicted from α, G_F, and M_Z by $\sim(8,14,25,45)$ MeV for $m_t=(91,150,200,250)$ GeV, respectively; i.e., in that range of m_t values they enhance the well-known perturbative corrections [3,16] by some 25 to 40%. Conversely, the value of m_t predicted from current measurements of M_W is increased by 1.6 to 3.3 GeV as M_W varies from 79.87 to 80.41 GeV.

ACKNOWLEDGMENTS

We are grateful to Michael Peskin and Thomas Teubner for making available to us their computer programs for evaluating the imaginary part of the Green's function, and to Riccardo Barbieri, Matteo Beccaria, Giuseppe Degrassi, Sergio Fanchiotti, Fred Jegerlehner, Hans Kühn, Alfred Mueller, and Peter Zerwas for very useful discussions. One of us (A.S.) would like to thank SISSA, Trieste, Italy, where part of his work on this problem was carried out, for the kind hospitality extended to him. This research was supported in part by the National Science Foundation under Grant No. PHY-9017585.

[1] R. E. Cutkosky, J. Math. Phys. **1**, 429 (1960).
[2] T. H. Chang, K. J. F. Gaemers, and W. L. van Neerven, Nucl. Phys. **B202**, 407 (1982).
[3] B. A. Kniehl, Nucl. Phys. **B347**, 86 (1990).
[4] B. A. Kniehl and J. H. Kühn, Phys. Lett. B **224**, 229 (1989); Nucl. Phys. **B329**, 547 (1990).
[5] A. Sirlin, Phys. Rev. D **22**, 971 (1980).
[6] H. Burkhardt, F. Jegerlehner, G. Penso, and C. Verzegnassi, Z. Phys. C **43**, 497 (1989).
[7] B. A. Kniehl, M. Krawczyk, J. H. Kühn, and R. G. Stuart, Phys. Lett. B **209**, 337 (198).
[8] F. Jegerlehner, Z. Phys. C **32**, 195 (1986).
[9] J. H. Kühn and P. M. Zerwas, Phys. Rep. **167**, 321 (1988).
[10] V. S. Fadin and V. A. Khoze, Pis'ma Zh. Eksp. Teor. Fiz. **46**, 417 (1987) [JETP Lett. **46**, 525 (1987)]; Yad. Fiz. **48**, 487 (1988) [Sov. J. Nucl. Phys. **48**, 309 (1988)].
[11] W. Kwong, Phys. Rev. D **43**, 1488 (1991).
[12] M. J. Strassler and M. E. Peskin, Phys. Rev. D **43**, 1500 (1991).
[13] B. A. Kniehl, J. H. Kühn, and R. G. Stuart, Phys. Lett. B **214**, 621 (1988); B. A. Kniehl, Comput. Phys. Commun. **58**, 293 (1990).
[14] CDF Collaboration, F. Abe *et al.*, Phys. Rev. Lett. **68**, 447 (1992); Phys. Rev. D **45**, 3921 (1992).
[15] F. Halzen and B. A. Kniehl, Nucl. Phys. **B353**, 567 (1991).
[16] A. Djouadi and C. Verzegnassi, Phys. Lett. B **195**, 265 (1987); A. Djouadi, Nuovo Cimento A **100**, 357 (1988).
[17] J. J. van der Bij and F. Hoogeveen, Nucl. Phys. **B283**, 477 (1987).
[18] R. Barbieri, M. Beccaria, P. Ciafaloni, G. Curci, and A. Viceré, Phys. Lett. B **288**, 95 (1992).
[19] B. W. Lee, in *Proceedings of the 16th International Conference on High Energy Physics,* Chicago, Illinois, 1972, edited by J. D. Jackson and A. Roberts (National Accelerator Laboratory, Batavia, 1972), Vol. IV, p. 266; D. A. Ross and M. Veltman, Nucl. Phys. **B95**, 135 (1975); M. Veltman, *ibid.* **B123**, 89 (1977); M. S. Chanowitz, M. A. Furman, and I. Hinchliffe, Phys. Lett. **78B**, 285 (1978); P. Q. Hung and J. J. Sakurai, Nucl. Phys. **B143**, 81 (1978); **B148**, 538(E) (1979).
[20] B. A. Kniehl and A. Sirlin, Nucl. Phys. **B371**, 141 (1992).
[21] W. J. Marciano and A. Sirlin, Phys. Rev. D **22**, 2695 (1980).
[22] A. Sommerfeld, *Atombau und Spektrallinien* (Vieweg, Braunschweig, 1944), Vol. 2, p. 130.
[23] G. Grunberg, Phys. Lett. **95B**, 70 (1980); Phys. Rev. D **29**, 2315 (1984).
[24] P. M. Stevenson, Phys. Rev. D **23**, 2916 (1981); Nucl. Phys. **B203**, 472 (1982).
[25] M. A. Shifman, A. I. Vainshtein, and V. I. Zakharov, Nucl. Phys. **B147**, 385 (1979).
[26] B. Grinstein and M.-Y. Wang, Nucl. Phys. **B377**, 480 (1992).
[27] J. L. Richardson, Phys. Lett. **82B**, 272 (1979).
[28] S. Güsken, J. H. Kühn, and P. M. Zerwas, Phys. Lett. **155B**, 185 (1985); Nucl. Phys. **B262**, 393 (1985).
[29] K. Igi and S. Ono, Phys. Rev. D **33**, 3349 (1986).
[30] G. Altarelli, lecture delivered at the Workshop on QCD—20 Years Later, Aachen, Germany, 1992 (unpublished).
[31] M. Jeżabek and J. H. Kühn, Nucl. Phys. **B314**, 1 (1989).
[32] S. Fanchiotti, B. Kniehl, and A. Sirlin, Reports No. CERN-TH.6749/92 and No. NYU-Th-92/12/05, 1992 (unpublished).
[33] S. Fanchiotti and A. Sirlin, in *M.A.B. Bég Memorial Volume,* edited by A. Ali and P. Hoodbhoy (World Scientific, Singapore, 1991), p. 58.
[34] W. J. Marciano, Phys. Rev. D **29**, 580 (1984).
[35] F. Jegerlehner, in *Proceedings of the 1990 Theoretical Advanced Study Institute in Elementary Particle Physics,* Boulder, Colorado, 1990, edited by M. Cvetič and P. Langacker (World Scientific, Singapore, 1991), p. 476.
[36] R. Tanaka, lecture delivered at the XXVI International Conference on High Energy Physics, Dallas, Texas, 1992 (unpublished).
[37] Particle Data Group, K. Hikasa *et al.*, Phys. Rev. D **45**, S1 (1992), Part II.
[38] CDF Collaboration, F. Abe *et al.*, Phys. Rev. Lett. **65**, 2243 (1990); Phys. Rev. D **43**, 2070 (1991); UA2 Collaboration, J. Alitti *et al.*, Phys. Lett. B **276**, 354 (1992).